Partitioning and inhibition of hemoglobin-mediated lipid oxidation in chicken by components of black chokeberry press cake

Xueqing Lei[a], Zhaoyi Han[a], Longqi Chen[a], Ling Liu[a]*

[a]The College of Food Science, Shenyang Agricultural University, Shenyang, China

*Corresponding authors:

Ling Liu, liuling4568@163.com

The College of Food Science, Shenyang Agricultural University, Shenyang 110866, Dongling Street No.120, Shenyang, China

Abstract

Black chokeberry press cake (BCPC), a by-product of black chokeberry processing, is rich in antioxidants such as proanthocyanidin (PCA) and anthocyanin. In this study, the mechanism of antioxidants in BCPC against hemoglobin(Hb)-mediated lipid oxidation in chicken was elucidated. The result showed that BCPC inhibited Hb-mediated lipid oxidation in a concentration-dependent manner, with 15% BCPC exerting the best inhibitory effect. Liquid chromatography revealed that BCPC had high PCA, chlorogenic acid (CA), and neochlorogenic acid contents, in them CA exhibited higher inhibitory effect on Hb-mediated lipid oxidation. PCA and CA can form strong hydrogen bonding interactions with Hb active sites, which is beneficial for stabilizing heme in Hb pockets, reducing the transformation of oxyhemoglobin to methemoglobin, and thus delaying the release of heme; NCA is different from PCA and CA in that it seizes the binding site between globin and heme on Hb, leading to the detachment of heme from globin.

Keyword: By-product; Chlorogenic acid; Flavonoids; Molecular docking; Natural antioxidants; Neochlorogenic acid; Proanthocyanidins

1. Introduction

Lipid oxidation is the primary reason for the decrease in the quality of meat products, including aquatic products, livestock, and poultry. Lipid oxidation in meat results a rancid odor, deteriorates product color, and leads to oxide accumulation and loss of nutritional quality (Wu et al., 2022c). Therefore, controlling lipid oxidation is vital for maintaining meat and meat product quality.

Hemoglobin (Hb) is a pro-oxidant that can mediate lipid oxidation. Hb is a tetrameric protein comprising two α-chains and β-chains (α2β2), each with an iron protoporphyrin moiety (heme) located in the cavity of each globin chain. At post-mortem pH, iron protoporphyrin readily dissociates from globin and can get embedded within the phospholipid bilayer of the cell membrane; this facilitates the breakdown of preformed lipid hydroperoxides to generate alkoxyl and peroxyl groups for lipid oxidation (Wu et al., 2022b).

Black chokeberry is a shrub belonging to the Rosaceae family that is rich in polyphenols. Owing to its astringent taste, black chokeberry is generally not eaten raw; however, it is widely processed in the food industry for juices, syrups, jams, fruit teas, and dietary supplements (Sidor et al., 2019). Black chokeberry press cake (BCPC) is the residue or by-product and it is generally discarded directly during its processing, this treatment not only causes environmental pollution, but also leads to the waste of active polyphenols in BCPC. In fact, the cake pressing process is more conducive to the extraction of polyphenols (Witczak et al., 2021).

The literature has reported the antioxidant properties of black chokeberry both i*n*

vivo and *in vitro* (Gao et al., 2023; Hwang et al., 2014). However, only a few studies have reported the antioxidant effect of black chokeberry in meat products. Based on the promoting effect of Hb on lipid oxidation of meat, we hypothesize that BCPC has the ability to inhibit Hb oxidation and thus decrease lipid oxidation. Therefore, the objectives of this study were (i) to investigate the effect of BCPC on lipid oxidation in the Hb-mediated oxidative model using washed chicken muscle (WCM); (ii) to determine key antioxidant ingredients in BCPC and their effect on Hb autoxidation; and (iii) to elucidate which antioxidant ingredients of BCPC were most relevant to the reduction of lipid oxidation mediated by Hb.

2. Material and methods

2.1 Materials

Heparin, streptomycin sulfate, Sodium chloride, hydrogen chloride (HCl), sodium hydroxide (NaCl), sodium phosphate, sodium acetate, glacial acetic acid, 2,4,6-tripyridyl-S-triazine, potassium persulfate, ferrous chloride(III), ammonium ferrous sulfate ($NH_4Fe(SO_4)_2$), sodium carbonate, butanol, Folin-Ciocalteu reagent (1N), ethanol, chloroform, ammonium thiocyanate, ferrous chloride(II), methanol, potassium ferricyanide, trifluoroacetic acid, trichloroacetic acid (TFA) and thiobarbituric acid were purchased from Sinopharm Chemical Reagent Co., Ltd. (Shanghai, China). Tris, DPPH, ABTS, quercetin standard (purity>98%), chlorogenic acid standard (purity>98%), neochlorogenic acid standard (purity>98%), anthocyanin 3-O-glucoside standard (purity>98%), proanthocyanidin standard (purity>95%) and

tetraethoxypropane was purchased from Shanghai Macklin Biochemical Co., Ltd. (Shanghai, China). Water was purified by an ultra-pure water system from Shanghai Canrex Analytic Instrument Co., Ltd. (Shanghai, China). All other chemical reagents were of analytical grade or higher purity.

2.2 Preparation of WCM oxidation model

2.2.1 Preparation of WCM

The chicken breasts were obtained from fresh chicken (*Gallus gallus*) from Dadong Agricultural Market in Shenyang, Liaoning province, China. They were prepared and processed to obtain WCM according to Richards' method (Richards et al., 2002). After chicken breast was ground in a mincer, the mince was mixed with distilled deionized water at a ratio of 1:3. The mixture was stirred for 2 min and then incubated on ice for 15 min. After drained with gauze, the mince was washed twice with 50 mmol/L sodium phosphate buffer (pH 6.3) and homogenized with a T 25 high-speed disperser (IKA, Staufen, Germany) at 6,000 rpm. The mixture was incubated for 15 min after washing and centrifugated at 12,000 g for 20 min at 4°C. The precipitation was collected as WCM, and every 20 g of WCM was divided into sealed bags and frozen at -80°C before analysis. All steps were performed at 4°C.

2.2.2 Preparation of chicken hemolysate

The chicken hemolysate was performed by the method of Lei et al (2022). The heparinized chicken blood was mixed with four volumes of ice cold 0.9% NaCl in 1

mmol/L Tris (pH 8.0) and centrifuged at 700 g for 10 min. The plasma (supernatant) was removed, the precipitate (red cell) was washed with 10 volumes of ice cold 1 mmol/L Tris (pH 8.0) for three times. Then red cells were lysed in 3 volumes of 1 mmol/L Tris (pH 8.0) for 1 h on ice. One-tenth volume of 1 mol/L NaCl was added to remove stroma, and then centrifuged at 12,000 g for 15 min. All the steps were conducted at 4°C and the hemolysate was stored at -80°C before analysis.

2.2.3 Preparation of BCPC powder

Black chokeberrys were purchased from Huadian City, Jilin Province, China. They were squeezed by the juicer (H-300 Series, Hurom, Seoul, Republic of Korea), which could separate juice and peel. The BCPC is the by-product from juice production. BCPC was frozen dry at -40°C for 48 h, and then was grinded to powder by a high-speed grinder (Hangzhou Baijie Technology Co., Ltd, China) at a speed of 8000 rpm. Afterwards, the ground BCPC is sieved through a 300 mesh sieve, the coarse particles remaining on the sieve are discarded and the sieved BCPC powder storage in sealed bag at 4°C until subsequent analysis.

2.2.4 WCM oxidation model

The sample of oxidation model was prepared according to the method described by Lee et al. (2006) with minor revisions. The thawed 25g WCM was adjusted to pH 6.3 in a beaker by using 1.0 mol/L NaOH solution, and if needed 1.0 mol/L HCl. The original moisture content of the WCM was 86.7 ± 2.2%, and Milli-Q water was added

to reach 90%. Streptomycin sulfate stock solution (2% w/v) was added to give a final concentration of 0.02%. BCPC powder was added to the WCM oxidation models at 0%, 5%, 10%, and 15% by weight of WCM dry matter, respectively. Chicken hemolysate was thereafter added to a final concentration 25 μmol Hb/kg of WCM and the sample was transferred to the bottom of a 250 mL E-flask wrapped in aluminum foil (in dark). All steps were performed on ice and the final samples were stored on an ice bed in cooler bags. Sub-samples were taken from E-flasks every 2 days. Samples with the same concentration of BCPC added are grouped together, every group was conducted triplicate.

2.3 Lipid oxidation of WCM model

2.3.1 Peroxide value (PV)

Primary lipid oxidation was studied by measuring PV according to the ferric thiocyanate method as described by Sajib et al. (2022). The sample (1 g) was mixed with 10 mL ice-cold chloroform:methanol (2:1, v/v) containing 0.05% BHT (w/v) and homogenized at 7104 g for 30 s, then sample was added into 4 mL ice-cold 0.5% NaCl and vortexed for 30 s. The mixture was centrifugated at 3,000 g for 6 min at 4°C and the bottom phase (chloroform phase) was further analyzed for PV. The chloroform phase of 2 mL was mixed with 1.33 mL new ice-cold chloroform-methanol (1:1, v/v), 33.4 μL ammonium thiocyanate and 33.4 μL freshly iron (II) chloride, and the mixture was vortexed for 2-4 s and incubated for 20 min at room temperature. The mixture was finally analyzed at 500 nm by UV spectrometer. The cumene hydroperoxide was used

as standard curve at concentrations from 0 to 0.02 mmol/L. The PV was calculated and expressed as μmol cumene hydroperoxide/kg sample. ~~Three independent replicates of each treatment were determined every other day.~~ Sub-samples were taken from E-flasks every 2 days. Every group was conducted triplicate.

2.3.2 Anisidine value (AnV)

Anisidine value was determined in triplicate for each of the samples based on AOCS Official Method Cd 18-90 (1).

2.4 Measurement of redness loss

Procedures used have been described previously by Thiansilakul et al. (2012) with modifications. Redness loss was determined by Minolta CR-300 Chroma Meter (Minolta Camera Co., Osaka, Japan). The aperture size was 1 cm. A white calibration plate was used to calibrate the instrument. ~~Each sample was carried out in triplicate.~~ Every group was conducted triplicate.

2.5 Determination of total phenolic content (TPC)

TPC was evaluated by the Folin–Ciocalteu method with slight modifications as reported by Zhang et al. (2022). BCPC powder (0.1 g) was added into 10 mL extraction solution (methanol:H_2O+TFA, 70:30+1%) and vortexed for 15 s. The mixture was sonicated for 10 min, which was shaken after 5 and 10 min. The sample was incubated in a water bath (60°C, 100 rpm) for 30 min and vortexed for 15 s. After centrifugating

(5,000 g, 5 min, 4°C), the supernatant was collected. The precipitation was redissolved in 5 mL extraction solution and vortexed for 15 s. Afterwards, the sonication and centrifugation were repeated as above. The dilute sample (500 μL) was mixed with 50 μL Folin-Ciocalteu reagent, 200 μL distilled water and 250 μL saturated Na_2CO_3. After incubation at room temperature for 10 min at dark, the samples were centrifugetd at 15,000 g for 5 min at 4°C. The absorbance was recorded at 765 nm by UV spectrophotometer (Infinite M200 Pro Nano-quant, TECAN, Austria). The gallic acid was used as standard curve at concentrations from 0 to 0.71 mmol/L. The TPC was calculated and expressed as milligrams of gallic acid equivalent per gram of dry weight (mg GAE/g DW). ~~Three independent replicates of each treatment were determined.~~ Every group was conducted triplicate.

2.6 Antioxidant in BCPC powder analysis

2.6.1 Proanthocyanidins Measurement

The PCA content was evaluated by butanol-HCl assay with slight modifications as reported by Gao et al. (2023). Briefly, a 100 μL sample was mixed with 80 μL of ultra-pure water, 220 μL of MeOH, 2 mL of butanol-HCl solution (95:5 v/v), and 67 μL of $NH_4Fe(SO_4)_2$-HCl solution. The mixture was heated at 95°C for 40 min and cooled for 20 min, the unheated solution was used as control. The absorbance was recorded at 550 nm. The level of PCAs was represented as milligram proanthocyanidin B2 equivalents proportion in TPC (%). All trials were carried out in triplicate.

2.6.2 Polyphenols measurement

The qualitative analysis of polyphenols in BCPCs was carried out as described by Gao et al. (2023). Analysis of polyphenolic compounds in lingonberry was performed using ultra-high performance liquid chromatography with photodiode array (UPLC-PDA) (Shimadzu LC-8050, Japan). Briefly, the chromatographic column used was a Waters-C18 column (4.6mm×250mm, 5μm). Different polyphenols in BCPCs were separated by gradient elution. The mobile phase was composed of A (0.1% formic acid-water) and B (0.1% formic acid-acetonitrile). The gradient elution was as follows: (0-1) min 10% B, (1-3) min 10%-11% B, (3-5) min 11%-12% B, (5-28) min 12%-15% B, (28-54) min 15%-25% B, (54-63) min 25%-30% B, (63-68) min 30%-100% B, and (68-72) min 100%-10% B. The injection volume was 10 μL and the flow rate was 0.3 mL/min. The detection wavelengths for PDA were successively 350 nm. Chlorogenic acid, quercetin, and cyanidin-3-O-glucoside were used as standards for phenolic acids, flavanols, and anthocyanins, respectively. The content of polyphenolic compounds was determined by the corresponding peak area and calibration curves of the standards. ~~All trials~~ Every group was performed in triplicate.

2.7 *In vitro* antioxidant capacity

2.7.1 DPPH radical scavenging activity of BCPC

The DPPH test was conducted as Bujor et al (2018) with a little modification. Briefly, a 50 μL of 0.01 g/mL BCPC solution was mixed with 1.5 mL of 0.06 mmol/L DPPH solution in methanol and vortexed for 2-3 s. After incubation for 20 min, the mixture was recorded at 515 nm. The DPPH• concentration was calculated from a

calibration curve analyzed by linear regression. The percentage of %Inhibition was calculated as follows:

$$\%\text{Inhibition} = \frac{A_B - A_E}{A_B} \times 100$$

Where A_B is the absorbance of blank; A_E is the absorbance of samples.

2.7.2 Ferric ion reducing antioxidant power (FRPA)

The FRAP of BCPCs was measured according to the method as described by Chen et al. (2019). FRAP reagent was freshly prepared by mixing of sodium acetate in glacial acetic acid (300 mmol/L, pH 3.6), 10 mmol/L TPTZ in 40 mmol/L HCl and 20 mmol/L $FeCl_3$ at the ratio of 10:1:1 (v/v/v). the sample was mixed with 300 µL of FRAP reagent and incubated at 37°C for 15 min. The sample was measured at 593 nm using a UV spectrophotometer (Infinite M200 Pro Nano-quant, TECAN, Austria). A standard calibration curve from 0-2 µmol/L of $FeSO_4 \bullet 7H_2O$ was plotted. Results should be expressed as equivalent µmoles of Fe^{2+}/mL of the samples.

2.7.3 ABTS

The ABTS was performed by the method of Dudonné et al., (2009) with minor revisions. The stock ABTS solution was mixed with 1 mL of 7 mM ABTS and 10.1 µL of 245 mM potassium persulfate, and incubated overnight (12-16 h) at room temperature at dark. The sample and 100-fold diluted stock ABTS solutions were mixed at a ratio of 1:19 and the absorbance was recorded at 734 nm.

2.8 Spectral analysis of oxidation levels combined with oxyhemoglobin(oxyHb) and antioxidant components in BCPCs.

Measurements were performed according to the method of Wu et al. (2022) with slight modifications. Briefly, the standards of antioxidants were dissolved in ethanol to obtain a 5 mmol/L stock solution. The methemoglobin (metHb) was mixed with antioxidant standards and diluted 200-fold by 10 mmol/L Tris (pH 8.0). The mixture was stored at 2°C and determined every other day. The samples were analyzed by using a UV spectrophotometer from 510-700 nm.

2.9 Molecular docking

The structures of the docked compounds Chlorogenic-Acid, Neochlorogenic-acid, and Procyanidin-B2 come from the PubChem database (https://pubchem.ncbi.nlm.nih.gov), and then were imported into the Chem3D software. The MM2 module was used for optimization, energy minimization, and preservation. The file is used as the ligand molecule for molecular docking. The protein crystal structure of Hb (PDB ID: 1HBR) was obtained from the RCSB database (https://www.rcsb.org/). The protein was processed on the Maestro11.9 platform and process with Schrodinger's Protein Preparation Wizard, remove crystal water, add missing hydrogen atoms, repair missing bond information, and repair missing peptides. Finally perform energy minimization on the protein, and optimization of geometry. Molecular docking was performed by Covalent Docking in the Glide module of Schrödinger Maestro software. Protein processing utilizes the Protein Preparation Wizard module. Receptors were

preconditioned, optimized and minimized (constrained minimization using OPLS3e force fields). All molecules were prepared with the default settings of the LigPrep module. When screening in the Glide module, import the prepared receptors to specify the appropriate positions in the receptor mesh generation. Finally, the standard docking method (Standard Precision, SP) was used for molecular docking and screening.

2.10 Statistical analysis

All experiment of this study were statistically analyzed using SPSS 19.0 and significant differences between variables were determined using one-way analysis of variance (ANOVA). The sample was divided into three replicates, each of which was considered an experimental unit (n=3).

3. Results and discussion

3.1 The antioxidant capacity of BCPC in WCM

PV and AnV value were used to monitor the level of lipid oxidation (Figure 1). The contents of PV measured in WCM oxidation model with 0%, 5%, 10% and 15% BCPC at day 0 were 49.23 ± 3.25, 46.34±12.58, 45.77±2.21 and 44.65±1.05 μmol LHP/kg muscle, indicating that there no significantly differences ($p > 0.05$) in BCPC addition at the start of storage. During the ice storage, the PV of 0% BCPC initially increased and had achieved their maximum on day 4, which was significantly higher than the values at 5%, 10%, and 15% BCPC ($p < 0.05$). Similarly, the oxidation systems with 5% and 10% BCPC addition reached the highest oxidation values of 645 μmol LHP/kg and 345 μmol LHP/kg on day 6 and day 10, which were significantly higher than the values of other additions ($p < 0.05$), respectively. However, no significant lag phase was observed in WCM oxidation model in 15% BCPC group, with a low PV value (≤89.87 μmol LHP/kg) throughout storage. Also, the change of AnV aligned with the PV trend. These results indicated that BCPC exhibits a strong inhibitory effect on Hb-mediated lipid oxidation, with a concentration-dependent antioxidant capacity. BCPC of black chokeberry contains high polyphenol, TPC, flavonoid contents, especilly PCA contents were four-fold higher than those of the blueberry extract (Hwang et al., 2014; Zhao et al., 2022). The phenolic hydroxyl groups in polyphenols can reduce the formation of metHb, thereby decreasing the oxidative activity of Hb (Wu et al., 2022a). Moreover, phenolic compounds could scavenge free radicals and form a chelate with transition metal catalysts to limit lipid oxidation (Zamora and Hidalgo, 2016).

The addition amounts of TPC and BCPC are concentration-dependent, and the initial value of TPC in the WCM oxidation system adding 15% BCPC is 0.45 mg GAE/g DW. With the extension of storage time, TPC gradually decreased and stabilized at around 0.15-0.2 mg GAE/g DW. Until the end of storage, the TPC in the WCM oxidation system of 5% BCPC, 10% BCPC and 15% BCPC decreased 53.57%, 67.65% and 62.22%, respectively (Figure 1C). TPC was associated with a* value, which also decreased during the storage period (Figure 1D). Notably, the a* value of 5% BCPC was lower than that of 0% BCPC; this may be because BCPC addition darkened the color of the WCM model. With an increase in BCPC concentration, the a * values of 10% and 15% BCPC exceed those with 0% BCPC. In the present study, the red color of a* value was primarily derived from phenols and Hb. The red loss is partly due to the transition from oxyHb to methb, but phenolics slow down the red loss by hindering the process of hydrogen peroxide-mediated oxidation of oxyHb to metHb (Wu et al., 2022a). The other part of the loss of red color is due to the degradation of TPC with prolonged storage, and also the involvement of phenolic hydroxyl groups in anthocyanins in the chain reaction of lipids, which also reduces the anthocyanin content (Ferreres et al., 1996).

3.2 BCPC antioxidant capacity *in vitro*

The antioxidant capacity of BCPC in the WCM oxidation model may be involved in free radical scavenging. TPC represents the content of phenol hydroxyl groups in antioxidants. FRAP, DPPH, and ABTS assays were performed to measure the iron-

reducing ability, DPPH scavenging ability, and ABTS free radical scavenging ability, respectively (Blainski et al., 2013; Hwang et al., 2014; Valverde Malaver et al., 2018). As Figure 2A shown, TPC and FRAP proportionally increased with an increase in BCPC concentration. In Figure 2B, when the BCPC concentration was increased from 5.0 to 20.0 μg/mL, ABTS decolorization rapidly increased and then reached a plateau, with a scavenging rate of approximately 100%. DPPH inhibition also exhibited the same trend, but the maximum plateau value was achieved at approximately 80%. The *in vitro* antioxidant capacity of FRAP, DPPH, and ABTS is related to their antioxidant activity, which may depend on TPC (Hwang et al., 2014). The above results indicated that BCPC had strong antioxidant and free radical scavenging ability. Therefore, the phenolic monomers in BCPC were further investigated by UV-Vis spectroscopy and UPLC-PDA.

3.3 Identification of the antioxidants in BCPC and their inhibitory of Hb auto-oxidation

UPLC-MS analysis was performed to determine the types of polyphenol extracts in BCPC. Chlorogenic acid (CA, peak 4) and neochlorogenic acid (NCA, peak 3) were identified as the two higher content substances (Figure 3). In addition to these two antioxidants, PCA was identified as the major polyphenol in black chokeberry. In our study, the PCA was accounted for 56.7% of TPC.

Polyphenols can reduce the pro-oxidant activity of Hb by reducing Hb from pro-oxidant metHb to oxyHb (Wu et al., 2022c). Figure 4 illustrates the UV-visible

spectrum of chicken metHb with or without PCA/CA/NCA after 6 days of incubation. The spectrum displayed a significant trough and peak on day 0. As the storage time prolongs, Hb-PCA and Hb-CA still have obvious peaks and troughs on the 6th day of storage, while the absorption curve of Hb-NCA tends to be flat, indicating that Hb has been denatured. PCA was used as a reducing and chelating agent to maintain Hb in a ferrous state, and that the inhibitory effect of PCA as a reducing agent on Hb-mediated lipid oxidation was higher than that of PCA as a chelating agent (Maestre et al., 2009). Similarly, CA maintained the ferrous state of Hb by chelating with iron ions and effectively reduce the production of •OH triggered by iron ions (Yang et al., 2021). In Figure 4, the initial absorbance baseline of Hb-PCA was higher than that of Hb-CA and Hb-NCA, which may be because PCA is purple, therefore it increased the baseline value. These results indicate that PCA and CA can delay Hb-mediated lipid oxidation by inhibiting the oxidation of oxyHb to metHb, but NCA cannot effectively inhibit Hb autoxidation.

3.4 The mechanism of molecular docking between CA, NCA, PCA-B2 and Hb

Figure 5 demonstrates that the interaction and action sites between CA, NCA, PCA-B2 and Hb. CAs are esters formed between caffeic and quinic acids (Xu et al., 2012). As Figure 5A shown, hydroxyl groups on CA form hydrogen bonds with aspartate (ASP,126), serine (SER,130), valine (VAL,34), tyrosine (TYR,140), and glutamate (GLU,138). Compared with PCA-B2 (Mm=578.52), CA's molecular mass (Mm=354.31) is smaller. These smaller ligands typically bind better to the cavity site

(Kamenik et al., 2021), thus CA prone to bind with Hb's cavity, hindering the solvent entry. Once the solvent enters the cavity, it will reduce the affinity of chicken Hb to oxygen, and further triggers the protonation of distal histidine and weakens the iron binding between the imidazole moiety and hemoglobin, leading to the dissociation of globin and heme (Lei et al., 2022b).

Studies have reported the antioxidant capacity of NCA, comparatively a less-studied isomer of CA (Navarro-Orcajada et al., 2021; Rop et al., 2010). In Figure 5B, NCA also bound on Hb with six amino acid by hydroxyl groups. Notably, NCA binds to lysine at position 99 (E10) of Hb, this position is a key site in the control of the Hb cavity (Wu et al., 2017; Yin et al., 2017). This binding may lead to detachment of the porphyrin ring from the bead proteins, and the iron ions on the porphyrin ring can trigger lipid oxidation via the Fenton reaction with H_2O_2, producing the highly oxidizing hydroxyl radical (Maestre et al., 2009).

The inconsistent reducing and chelating abilities of CA, NCA and PCA to Hb are related to their structures. Molecular docking of CA, NCA and PCA with Hb was performed to study the impact of their combination with Hb on the structure of Hb. From a chemical point of view, proanthocyanidins are an oligomeric polyphenol compound, most of which are oligomers of catechin, epicatechin and their gallic acid esters. Proanthocyanidins are mainly divided into type A, type B and type C according to the linking methods of catechin, epicatechin and their gallic acid esters. Among them, B2 is a common type of flower found in *Sorbus nigra. cyanins* (Sidor et al., 2019; Esatbeyoglu & Winterhalter, 2010; Wu et al., 2004), so PCA-B2 was used for molecular

docking experiments in this study.

PCA forms stable compounds with other substances with the help of hydrogen bonds (Nie et al., 2023). As Figure 5C shown, PCA-B2 bound to Hb via hydrogen bonding to leucine (LEU, 2), valine (VAL, 34), serine (SER, 130), alanine (ALA, 134), glutamate (GLU, 138), respectively. These hydrogen bonds can help PCA-B2 to bind in the Hb cavity, thus PCA-B2 blocks solvent entry into the Hb cavity and delays the oxidation of Hb from the oxyHb to the metHb, further inhibits Hb-mediated lipid oxidation. Remarkably, among the six amino acid sites where PCA-B2 binds to Hb, ALA, VAL and LEU are all hydrophobic amino acids, which may lead to form a more hydrophilic environment around the Hb cavity, causing the solvent to enter the Hb cavity and accelerating lipid oxidation (Wu et al., 2017). The investigation of Fan et al. (2022) also found that PCA-B2 was able to change the conformation of bovine α-lactalbumin in the hydrophobic cavity by hydrogen bonding to further form a stable structure.

3.5 Inhibition of lipid oxidation in WCM model by PCA, CA, and NAC

In order to further verify whether PCA, CA and NCA can inhibit Hb-mediated lipid oxidation, the contents of PCA, CA and NCA in 15% BCPC were used as the benchmark and were added to the WCM model respectively, and then lipid oxidation analysis was performed. Results of WCM oxidation model with/without the three antioxidants are demonstrated in Figure 6. As shown in Figure 6A, 0% BCPC group reached the highest oxidation value of 251.75 μmol LHP/kg muscle on 4d, while the

NCA added group also reached the highest oxidation value on 4d, but the peak oxidation value was only 111.29 μmol LHP/kg muscle, indicating that although NCA did not delay the arrival of the lipid oxidation peak, it can inhibit the intensity of the lipid oxidation peak. The groups added with PCA and CA reached the highest oxidation peaks on day 6 and day 8 respectively, which were 97.90 μmol LHP/kg muscle and 103.87 μmol LHP/kg muscle. The mixed group of three antioxidants reached the highest oxidation peak on day 10. The results of AnV were consistent with those of PV (Figure 6B). All antioxidants could significantly inhibit the formation of PV, but could not significantly reduce the AnV peak ($p > 0.05$).

CAs inhibit lipid oxidation by donating hydrogen atoms to reduce free radicals. After donating a hydrogen atom, CA is oxidized to form the respective phenoxy groups, which are rapidly stabilized via resonance stabilization (Liang and Kitts, 2016). Cao et al. (2019) reported that CA acted as a hydrogen donor and inhibited lipid oxidation as well as maintained the color of fish flesh; furthermore, CA exerted an inhibitory effect on lipase and lipoxygenase activities because CA quenched the intrinsic fluorescence of the enzyme via static quenching. NCA as an isomer of CA, also has a similarly strong antioxidant capacity (Thurow and Lee, 2012), however, they show a different antioxidant capacity in WCM oxidation model. It might be due to that the differences between CA and NCA are partially because NCA content was less than CA content in the WCM model, which NCA content was 90% of CA content in BCPC. Furthermore, NCA cannot be easily distributed into the lipid phase because of its hydrophilic nature (Navarro-Orcajada et al., 2021). In addition, NCA can be easily degraded under neutral

conditions (the pH of the WCM model is 7); this may be one of the reasons why NCA has worse antioxidant capacity than CA (Wang, 2021).

4. Conclusions

BCPC, as an agricultural by-product, is rich in polyphenols. in this study, BCPC showed significantly inhibition capacity to lipid oxidation in chicken. PCA, CA and NCA were found to be the most abundant polyphenols in BCPC. Among them, PCA and CA can form strong hydrogen bond interactions with the Hb active site, which is beneficial to stabilizing the heme in the Hb pocket, reducing the transformation of oxyHb to metHb, thereby delaying the release of heme; NCA differs from PCA and CA in that it seizes the binding site between globin and heme on Hb, causing heme to detach from globin. Comparison of the three antioxidant components in the WCM oxidation model of lipid oxidation revealed that the antioxidant capacity of the three mixtures, CA, PCA and NCA, was in descending order of strength.

Acknowledge

This research was support by Applied Basic Research Program project, Liaoning Provincial, China (No. 2023JH2/101300127).

References

AOCS, Official Methods and Recommended Practices of the American Oil Chemists' Society, 4th edn., AOCS Press, Cham- paign, Additions and Revisions, Method Cd 18–90 (1992).

Blainski, A., Lopes, G., de Mello, J., 2013. Application and Analysis of the Folin Ciocalteu Method for the Determination of the Total Phenolic Content from Limonium Brasiliense L. Molecules 18, 6852–6865. https://doi.org/10.3390/molecules18066852

Bujor, O.-C., Ginies, C., Popa, V.I., Dufour, C., 2018. Phenolic compounds and antioxidant activity of lingonberry (Vaccinium vitis-idaea L.) leaf, stem and fruit at different harvest periods. Food Chemistry 252, 356–365. https://doi.org/10.1016/j.foodchem.2018.01.052

Cao, Q., Du, H., Huang, Y., Hu, Y., You, J., Liu, R., Xiong, S., Manyande, A., 2019. The inhibitory effect of chlorogenic acid on lipid oxidation of grass carp (Ctenopharyngodon idellus) during chilled storage. Food Bioprocess Technol.

Chen, W., Wang, W., Ma, X., Lv, R., Balaso Watharkar, R., Ding, T., Ye, X., Liu, D., 2019. Effect of pH-shifting treatment on structural and functional properties of whey protein isolate and its interaction with (−)-epigallocatechin-3-gallate. Food Chemistry 274, 234–241. https://doi.org/10.1016/j.foodchem.2018.08.106

Dudonné, S., Vitrac, X., Coutière, P., Woillez, M., Mérillon, J.-M., 2009. Comparative Study of Antioxidant Properties and Total Phenolic Content of 30 Plant Extracts of Industrial Interest Using DPPH, ABTS, FRAP, SOD, and ORAC Assays. J. Agric. Food Chem. 57, 1768–1774. https://doi.org/10.1021/jf803011r

Esatbeyoglu, T., Winterhalter, P., 2010. Preparation of Dimeric Procyanidins B1, B2, B5, and B7 from a Polymeric Procyanidin Fraction of Black Chokeberry (Aronia melanocarpa). J. Agric. Food Chem. 58, 5147–5153. https://doi.org/10.1021/jf904354n

Fan, Y., 2022. Investigation of binding interaction between bovine α-lactalbumin and procyanidin B2 by spectroscopic methods and molecular docking. Food Chemistry.

Ferreres, F., Gil, M.I., Tomás-Barberán, F.A., 1996. Anthocyanins and flavonoids from shredded red onion and changes during storage in perforated films. Food Research International 29, 389–395. https://doi.org/10.1016/0963-9969(96)00002-6

Gao, N., Si, X., Han, W., Gong, E., Shu, C., Tian, J., Wang, Y., Zhang, J., Li, Binxu, Li, Bin, 2023. The contribution of different polyphenol compositions from chokeberry produced in China to cellular antioxidant and antiproliferative activities. Food Science and Human Wellness 12, 1590–1600. https://doi.org/10.1016/j.fshw.2023.02.018

H Wu, J.Y.J.Z.M.P.R., 2017. Factors Affecting Lipid Oxidation Due to Pig and Turkey Hemolysate. Journal of Agricultural and Food Chemistry 65, 8011–8017.

Hwang, S.J., Yoon, W.B., Lee, O.-H., Cha, S.J., Kim, J.D., 2014. Radical-scavenging-linked antioxidant activities of extracts from black chokeberry and blueberry cultivated in Korea. Food Chemistry 146, 71–77. https://doi.org/10.1016/j.foodchem.2013.09.035

Kamenik, A.S., Singh, I., Lak, P., Balius, T.E., Liedl, K.R., Shoichet, B.K., 2021. Energy penalties enhance flexible receptor docking in a model cavity. Proc. Natl. Acad. Sci. U.S.A. 118, e2106195118. https://doi.org/10.1073/pnas.2106195118

Lee, C.-H., Krueger, C.G., Reed, J.D., Richards, M.P., 2006. Inhibition of hemoglobin-mediated lipid oxidation in washed fish muscle by cranberry components. Food Chemistry 99, 591–599. https://doi.org/10.1016/j.foodchem.2005.08.027

Lei, X., Qin, Z., Ye, B., Guo, F., Wu, Y., Liu, L., 2022a. Interaction between secondary lipid

oxidation products and hemoglobin with multi-spectroscopic techniques and docking studies. Food Chemistry 394, 133497. https://doi.org/10.1016/j.foodchem.2022.133497

Lei, X., Qin, Z., Ye, B., Wu, Y., Liu, L., 2022b. Effect of pH on lipid oxidation mediated by hemoglobin in washed chicken muscle. Food Chemistry 372, 131253. https://doi.org/10.1016/j.foodchem.2021.131253

Liang, N., Kitts, D.D., 2016. Role of Chlorogenic Acids in Controlling Oxidative and Inflammatory Stress Conditions.

Maestre, R., Pazos, M., Iglesias, J., Medina, I., 2009. Capacity of Reductants and Chelators To Prevent Lipid Oxidation Catalyzed by Fish Hemoglobin. J. Agric. Food Chem. 57, 9190–9196. https://doi.org/10.1021/jf901727x

Navarro-Orcajada, S., Matencio, A., Vicente-Herrero, C., García-Carmona, F., López-Nicolás, J.M., 2021. Study of the fluorescence and interaction between cyclodextrins and neochlorogenic acid, in comparison with chlorogenic acid. Scientific Reports.

Nie, F., Liu, L., Cui, J., Zhao, Y., Zhang, D., Zhou, D., Wu, J., 2023. Oligomeric Proanthocyanidins: An Updated Review of Their Natural Sources, Synthesis, and Potentials.

Richards, M.P., Modra, A.M., Li, R., 2002. Role of deoxyhemoglobin in lipid oxidation of washed cod muscle mediated by trout, poultry and beef hemoglobins. Meat Science 62, 157–163. https://doi.org/10.1016/S0309-1740(01)00242-X

Rop, O., Mlcek, J., Jurikova, T., Valsikova, M., Sochor, J., Reznicek, V., Kramarova, D., 2010. Phenolic content, antioxidant capacity, radical oxygen species scavenging and lipid peroxidation inhibiting activities of extracts of five black chokeberry (Aronia melanocarpa (Michx.) Elliot) cultivars. Journals of Medicinal Plants Research.

Sajib, M., Langeland, M., Undeland, I., 2022. Effect of antioxidants on lipid oxidation in herring (Clupea harengus) co-product silage during its production, heat-treatment and storage. Sci Rep 12, 3362. https://doi.org/10.1038/s41598-022-07409-8

Sidor, A., Drożdżyńska, A., Gramza-Michałowska, A., 2019. Black chokeberry (Aronia melanocarpa) and its products as potential health-promoting factors - An overview. Trends in Food Science & Technology 89, 45–60. https://doi.org/10.1016/j.tifs.2019.05.006

Thiansilakul, Y., Benjakul, S., Park, S.Y., Richards, M.P., 2012. Characteristics of myoglobin and haemoglobin-mediated lipid oxidation in washed mince from bighead carp (Hypophthalmichthys nobilis). Food Chemistry 132, 892–900. https://doi.org/10.1016/j.foodchem.2011.11.060

Thurow, T., 2012. Effect of Chlorogenic Acid and Neochlorogenic Acid on Human Colon Cancer Cells.

Valverde Malaver, C.L., Colmenares Dulcey, A.J., Isaza Martínez, J.H., 2018. Comparison of DPPH Free Radical Scavenging, Ferric Reducing Antioxidant Power (FRAP), and Total Phenolic Content of Two Meriania Species (Melastomataceae). RC 19, 8. https://doi.org/10.25100/rc.v19i2.6271

Verstraeten, S.V., Keen, C.L., Schmitz, H.H., Fraga, C.G., Oteiza, P.I., 2003. FLAVAN-3-OLS AND PROCYANIDINS PROTECT LIPOSOMES AGAINST LIPID OXIDATION AND DISRUPTION OF THE BILAYER STRUCTURE. Free Radical Biology & Medicine 84–92.

Viljanen, K., Kylli, P., Kivikari, R., Heinonen, M., 2004. Inhibition of Protein and Lipid Oxidation in Liposomes by Berry Phenolics. J. Agric. Food Chem 52, 7419−7424.

Wang, D., 2021. Degradation kinetics and isomerization of 5- O -caffeoylquinic acid under

ultrasound: Influence of epigallocatechin gallate and vitamin C. Food Chemistry.

Witczak, T., Stępień, A., Gumul, D., Witczak, M., Fiutak, G., Zięba, T., 2021. The influence of the extrusion process on the nutritional composition, physical properties and storage stability of black chokeberry pomaces. Food Chemistry 334, 127548. https://doi.org/10.1016/j.foodchem.2020.127548

Wu, H., Bak, K.H., Goran, G.V., Tatiyaborworntham, N., 2022a. Inhibitory mechanisms of polyphenols on heme protein-mediated lipid oxidation in muscle food: New insights and advances. Critical Reviews in Food Science and Nutrition 1–19. https://doi.org/10.1080/10408398.2022.2146654

Wu, H., Richards, M.P., Undeland, I., 2022b. Lipid oxidation and antioxidant delivery systems in muscle food. Comp Rev Food Sci Food Safe 21, 1275–1299. https://doi.org/10.1111/1541-4337.12890

Wu, H., Yin, J., Xiao, S., Zhang, J., Richards, M.P., 2022c. Quercetin as an inhibitor of hemoglobin-mediated lipid oxidation: Mechanisms of action and use of molecular docking. Food Chemistry 384, 132473. https://doi.org/10.1016/j.foodchem.2022.132473

Wu, X., Gu, L., Prior, R.L., McKay, S., 2004. Characterization of Anthocyanins and Proanthocyanidins in Some Cultivars of *Ribes* , *Aronia* , and *Sambucus* and Their Antioxidant Capacity. J. Agric. Food Chem. 52, 7846–7856. https://doi.org/10.1021/jf0486850

Xu, J.-G., Hu, Q.-P., Liu, Y., 2012. Antioxidant and DNA-Protective Activities of Chlorogenic Acid Isomers. J. Agric. Food Chem.

Yang, R., Tian, J., Liu, Y., Zhu, L., Sun, J., Meng, D., Wang, Z., Wang, C., Zhou, Z., Chen, L., 2021. Interaction mechanism of ferritin protein with chlorogenic acid and iron ion: The structure, iron redox, and polymerization evaluation. Food Chemistry 349, 129144. https://doi.org/10.1016/j.foodchem.2021.129144

Yin, J., Zhang, W., Richards, M.P., 2017. Attributes of lipid oxidation due to bovine myoglobin, hemoglobin and hemolysate. Food Chemistry 234, 230–235. https://doi.org/10.1016/j.foodchem.2017.04.182

Zamora, R., Hidalgo, F.J., 2016. The triple defensive barrier of phenolic compounds against the lipid oxidation-induced damage in food products. Trends in Food Science & Technology 54, 165–174. https://doi.org/10.1016/j.tifs.2016.06.006

Zhang, J., Abdollahi, M., Alminger, M., Undeland, I., 2022. Cross-processing herring and salmon co-products with agricultural and marine side-streams or seaweeds produces protein isolates more stable towards lipid oxidation. Food Chemistry 382, 132314. https://doi.org/10.1016/j.foodchem.2022.132314

Zhao, W., Cai, P., Zhang, N., Wu, T., Sun, A., Jia, G., 2022. Inhibitory effects of polyphenols from black chokeberry on advanced glycation end-products (AGEs) formation. Food Chemistry 392, 133295. https://doi.org/10.1016/j.foodchem.2022.133295

Figure captions

Figure 1. PV (A), AnV (B), TPC (C) and a* (D) of WCM mediated by hemolysate with different percentage BCPCs. 0%, 5%, 10% and 15% represent the added proportion of BCPC in the WCM oxidation systems, respectively.

Figure 2. Changes in TPC and anti-oxidation capacity (FRAP, DPPH and ABTS) in *in vitro* of BCPC powders with 0-80 μg/mL. Bars represent standard deviation (n = 3).

Figure 3. PAD chromatogram in polyphenols extract from BCPC at 350 nm. Peaks: Cyanidin 3-O-galactoside (1); Cyanidin 3-O-glucoside (2); Neochlorogenic acid (3); Chlorogenic acid (4); Quercetin 3-O-vicianoside (5); Quercetin 3-O-robinoside (6); Quercetin 3-O-rutinoside (7); Quercetin 3-O-galactoside (8); Quercetin 3-O-glucoside (9).

Figure 4. UV spectra (510–630 nm) of PCA(A), CA(B) and NCA(C) incubated with Hb in 10 mM tris buffer (pH 8.0) after 6 days storage on 4 °C.

Figure 5. Docking of chicken Hb (PdI: 1HBR) with chlorogenic acid (A), neochlorogenic acid (B) and procyanidin-B2 (C). The 3D structure of complex, the electrostatic surface of protein and the detail binding mode of ligand with protein were represented 1, 2 and 3 respectively.

Figure6. PV (A) and AnV (B) of WCM mediated by hemolysate with anti-oxidation components. Bars represent standard deviation (n = 3). Control represents the oxidation system without adding anti-oxidation components; PCA, CA, NCA and PCA+CA+NCA represents the WCM oxidation system with adding proanthocyanidins, chlorogenic acid, neochlorogenic acid and the mixture of proanthocyanidins, chlorogenic acid and neochlorogenic acid.

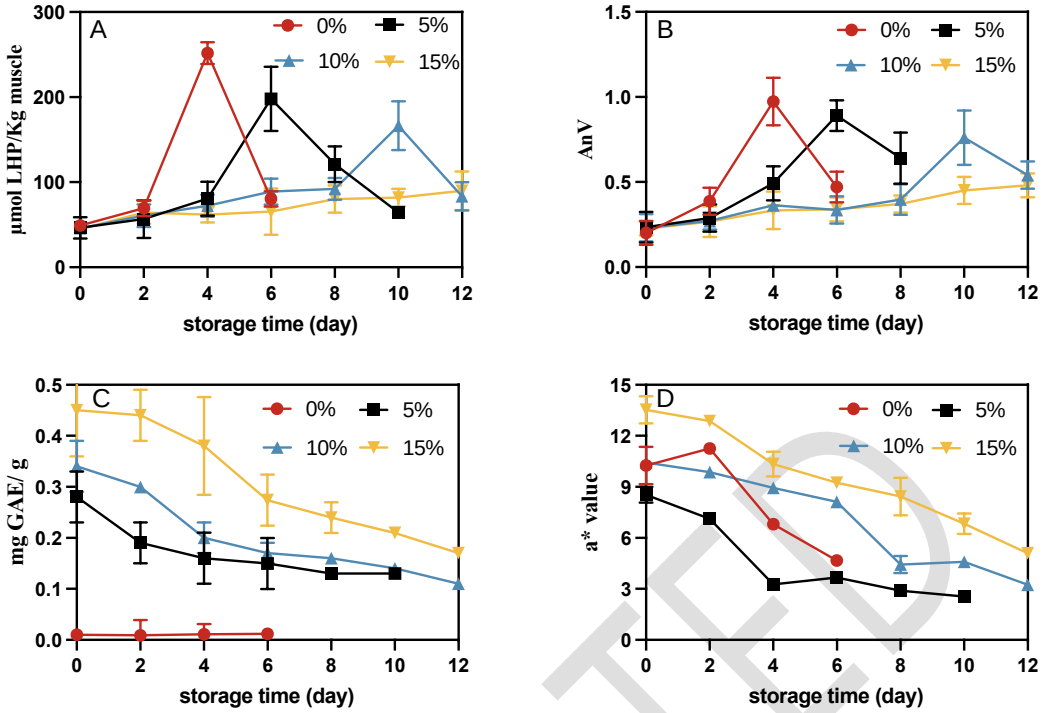

Figure 1

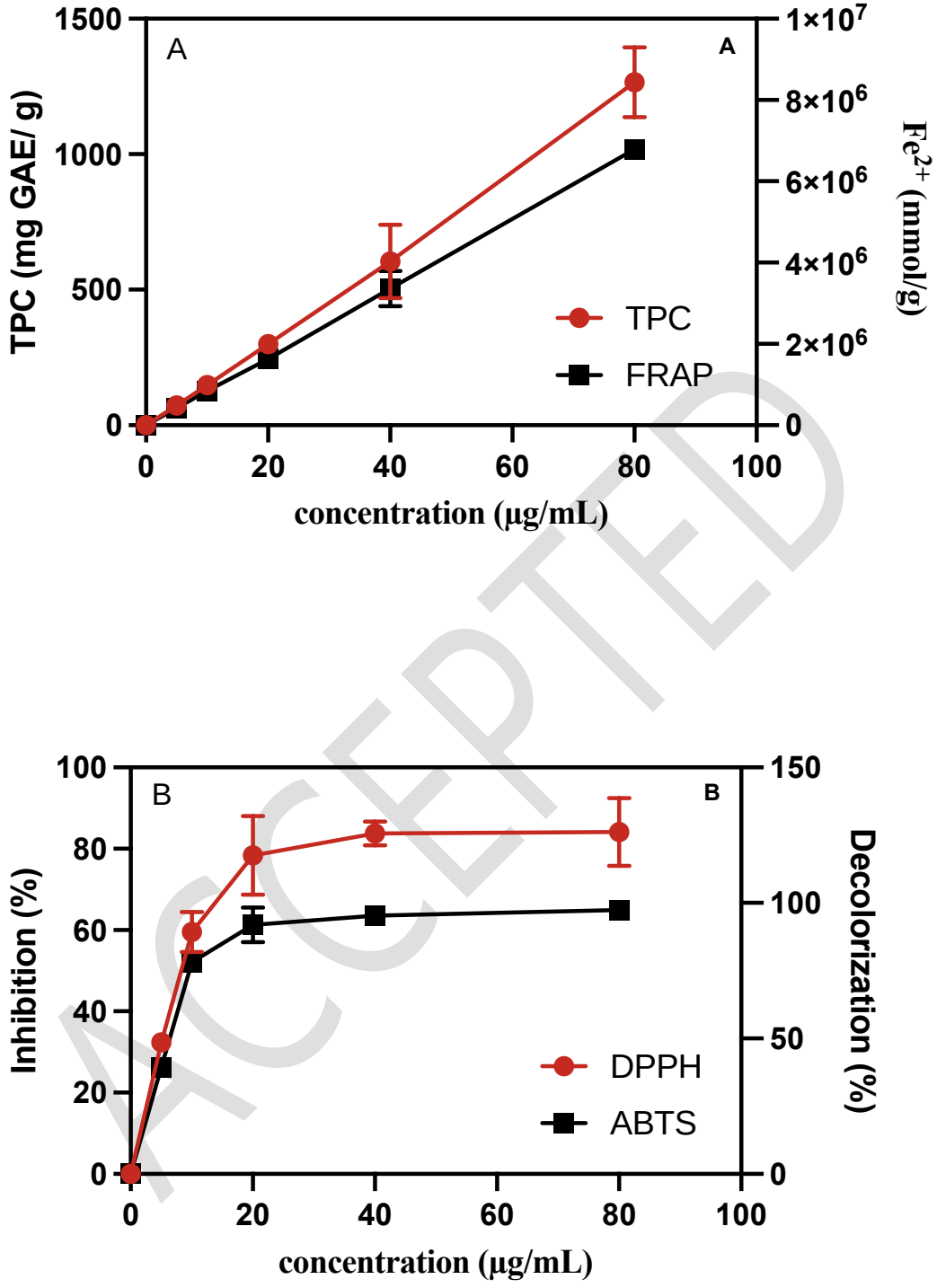

Figure 2

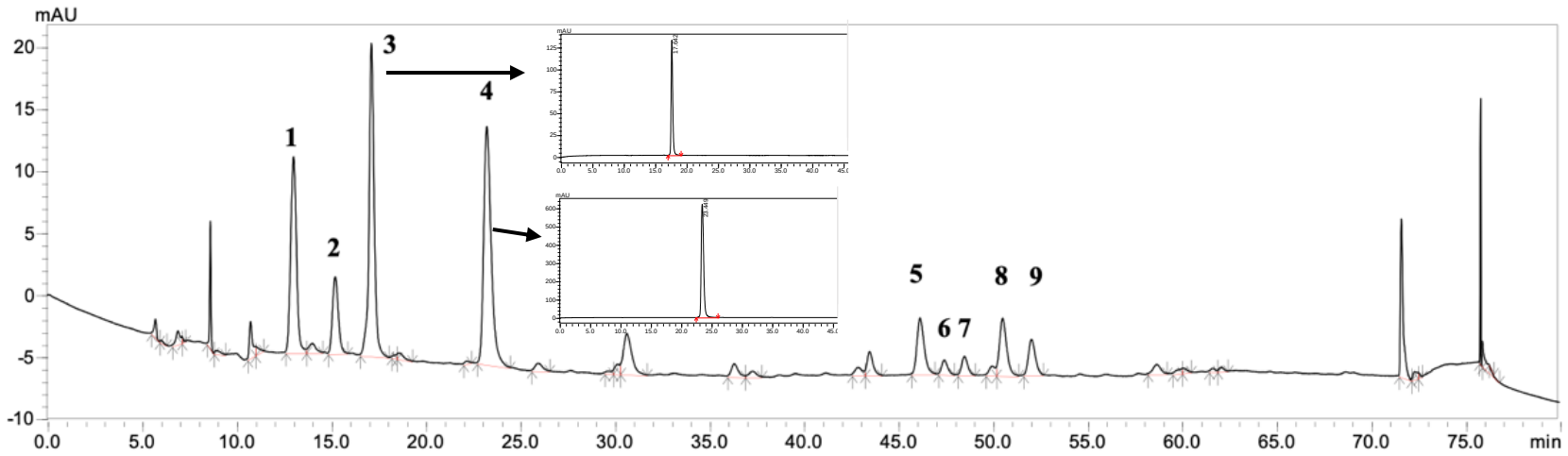
mAU
20
15
10
5
0
-5
-10
0.0
5.0
10.0
15.0
20.0
25.0
30.0
35.0
40.0
45.0
50.0
55.0
60.0
65.0
70.0
75.0
min
1
2
3
4
5
6 7
8
9

Figure 3

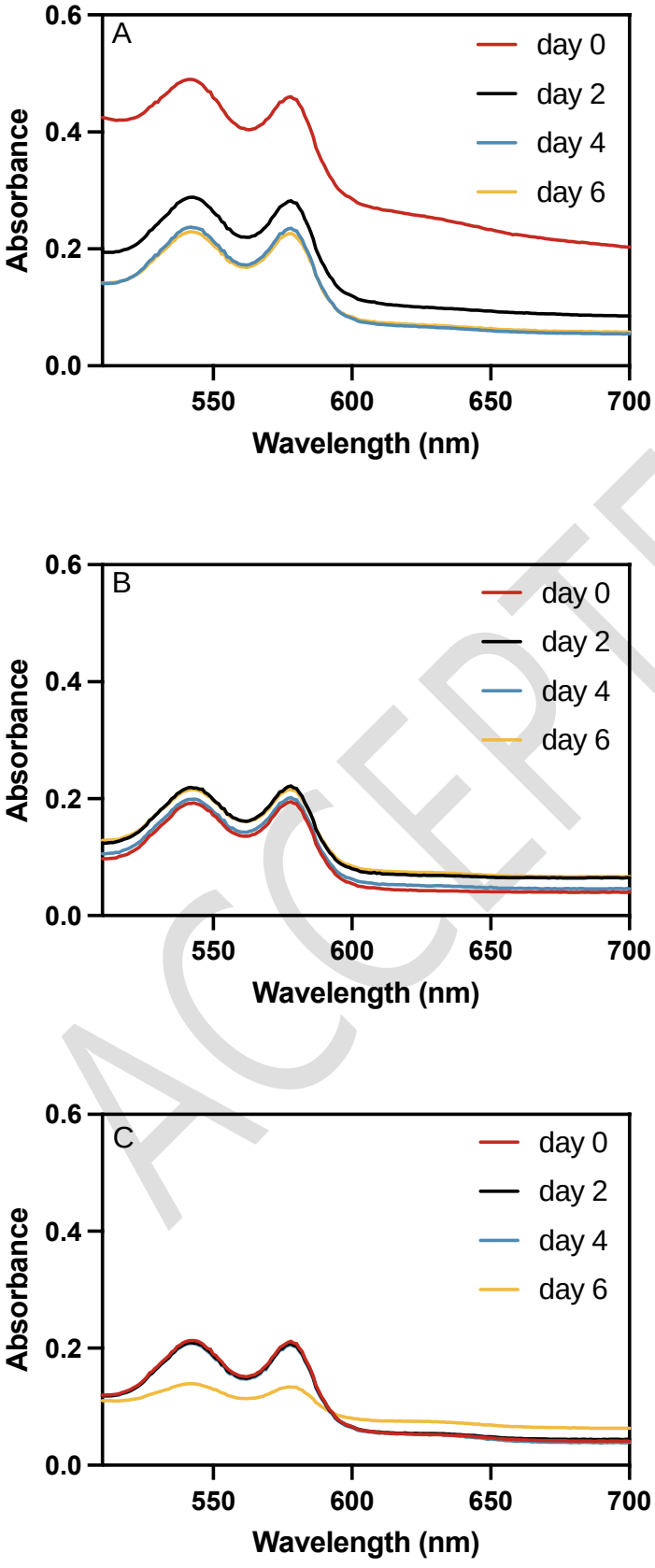

Figure 4

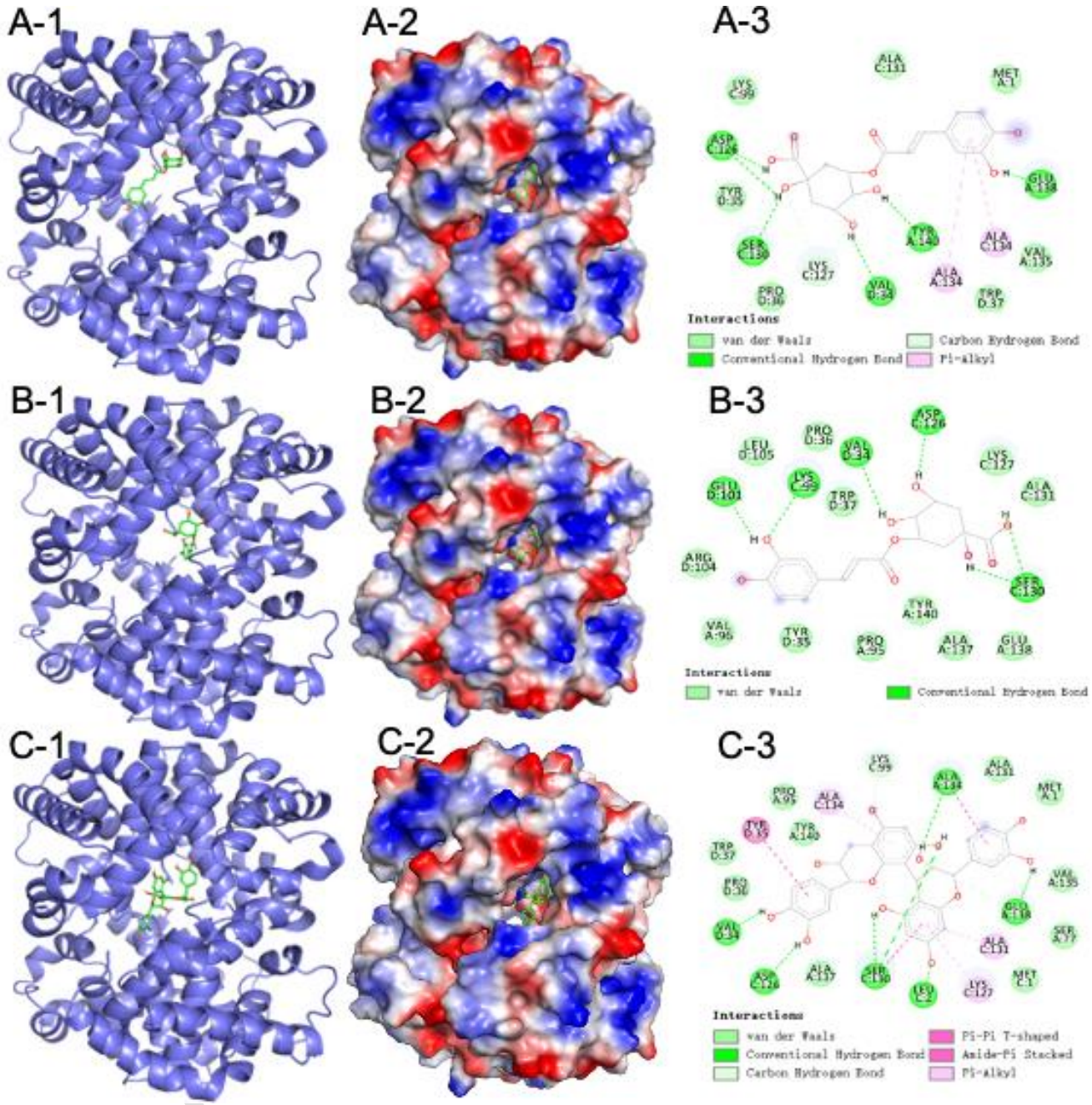
A-1
A-2
A-3
B-1
B-2
B-3
C-1
C-2
C-3
Interactions
van der Waals
Carbon Hydrogen Bond
Conventional Hydrogen Bond
Pi-alkyl
Interactions
van der Waals
Conventional Hydrogen Bond
Interactions
van der Waals
Pi-Pi T-shaped
Conventional Hydrogen Bond
Amide-Pi Stacked
Carbon Hydrogen Bond
Pi-alkyl

Figure 5

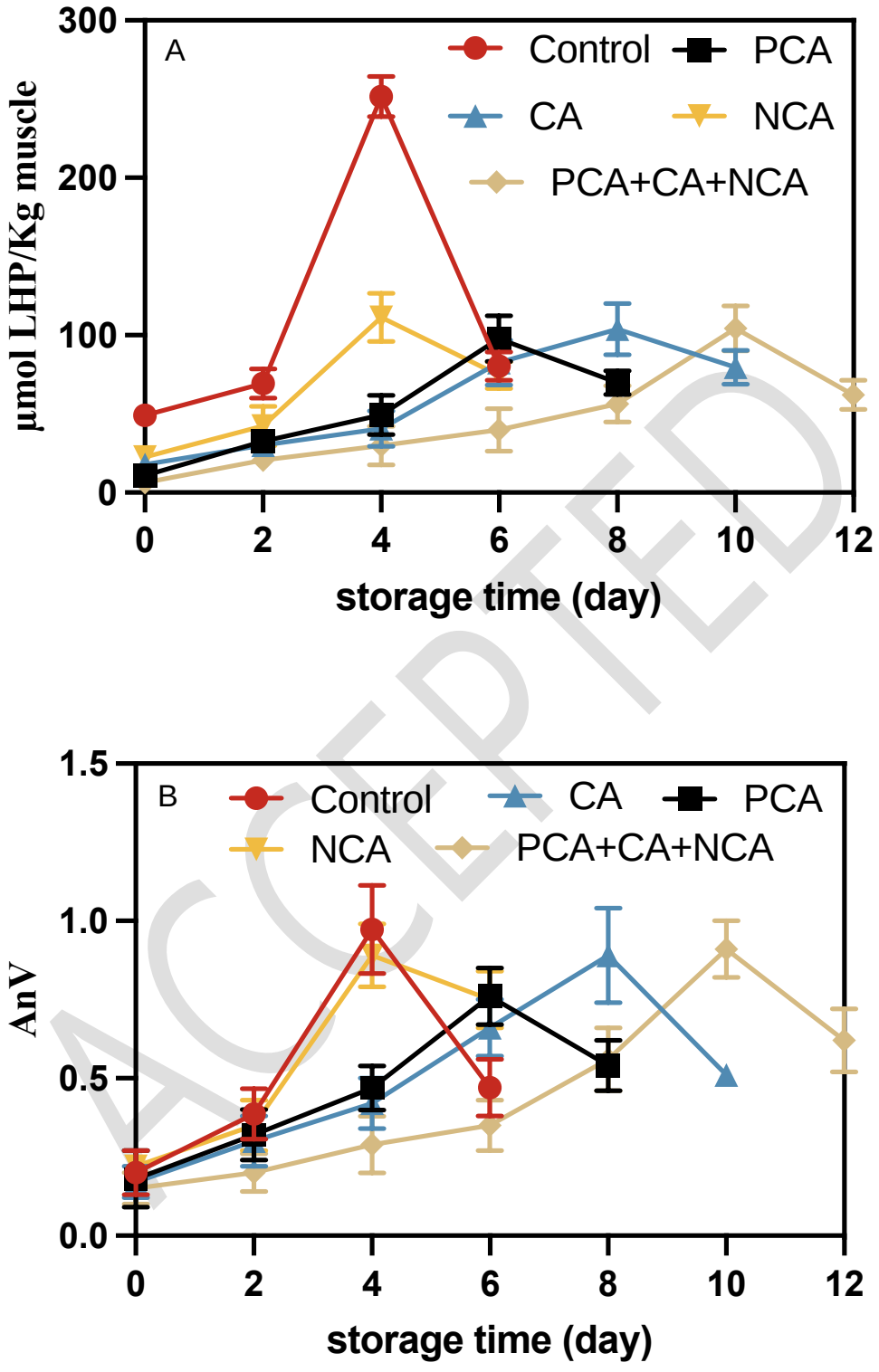

Figure 6

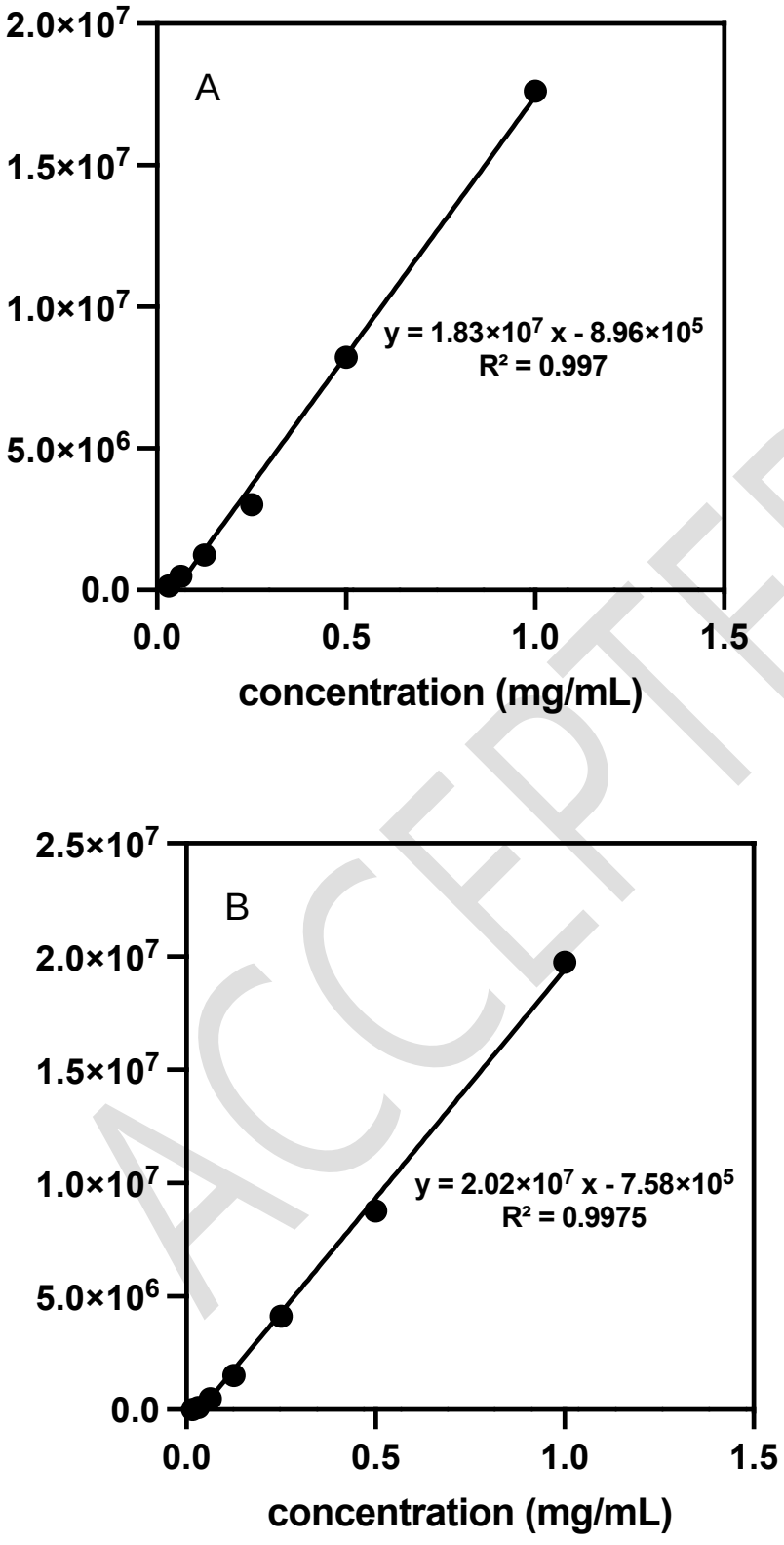

Figure S1 A standard calibration curve in the range from 0 µmol/L- 1mg/mL of chlorogenic acid (A) and neochlorogenic acid (B) were plotted.